Selecting optimum locations for co-located wave and wind energy farms. PART I: the Co-Location Feasibility index

S. Astariz[a1], G. Iglesias[b]

[a] *University of Santiago de Compostela, EPS, Hydraulic Eng., Campus Univ. s/n, 27002 Lugo, Spain.*

[b] *University of Plymouth, School of Marine Science and Engineering, Drake Circus, Plymouth PL4 8AA, UK.*

Abstract

Marine energy is poised to play a fundamental role in meeting renewable energy and carbon emission targets thanks to the abundant, and still largely untapped, wave and tidal resources. However, it is often considered difficult and uneconomical – as is usually the case of nascent technologies. Combining various renewables, such as wave and offshore wind energy, has emerged as a solution to improve their competitiveness and in the process overcome other challenges that hinder their development. The objective of this paper is to develop a new approach to identifying suitable sites for co-located wave and wind farms based on the assessment of the available resources and technical constraints, and to illustrate its application by means of a case study off the Danish coast – an area of interest for combining wave and wind energy. The method is based on an *ad hoc* tool, the Co-Location Feasibility (*CLF*) index, and is based on a joint characterisation of the wave and wind resources, which takes into account not only the available power but also the correlation between both resources and the power

[1] *Corresponding author*; email: sharay.astariz@usc.es; tel.: +34982823295; fax: +34982285926

variability. The analysis is carried out based on hindcast data and observations from 2005 to 2015, and using third-generation models of winds and waves – WAsP and SWAN, respectively. Upon selection and ranking, it is found that a number of sites in the study region are indeed suited to realising the synergies between wave and offshore wind energy. The approach developed in this work can be applied elsewhere.

Keywords: Wave energy; Wind energy; Co-located wind-wave farm; North Sea; Power variability; Cross-correlation factor.

Nomenclature

c (τ): cross-correlation factor between two variables for a time lag τ

c (0): instantaneous correlation

c.i.: confidence interval

CLFi: Co-Location Feasibility index of the *i*-th site point

CS: Case Study

E: energy density (Jm^{-3})

EMODnet: European Marine Observation and Data Network

ERDF: European Regional and Development Fund

g: gravity acceleration (ms^{-2})

H: height at which the wind speed is measured (m)

H_{m0}: significant wave height (m)

$\overline{H}_{m0}$: average significant wave height (m)

$H_{m0,max}$: maximum value of the significant wave height (m)

J: raw wave power (kWm^{-1})

$\overline{J}$: average raw wave power (kWm^{-1})

$m_{n:}$ spectral moment of order n

P: raw wind power (kWm^{-2})

$\overline{P}$: average raw wind power (kWm^{-2})

R^2: coefficient of determination

RMSE: Root Main Square Error

SWAN: Simulating WAves Nearshore

T_e: energy period (s)

$\overline{T_e}$: average energy period (s)

$T_{e,max}$: maximum energy period (s)

T_{mo1}: mean wave period (s)

U_w: wind speed (ms^{-1})

U_{10m}: wind speed at 10 m above the sea level (ms^{-1})

$\overline{U_{10m}}$: average wind speed 10 m above the sea level (ms^{-1})

$U_{10m,max}$: maximum value of the wind speed 10 m above the sea level (ms^{-1})

WAsP: Wind Atlas Analysis and Application Program

WEC: Wave Energy Converter

z: roughness length (m)

α_x: weighted factor of the parameter x when calculating the *CLF* index

ρ_a: air density (kgm^{-3})

ρ_w: sea water density (kgm^{-3})

θ: propagation direction (º)

$\theta_{wav,mean}$: mean wave direction (º)

$\theta_{wind,mean}$: mean wind direction (º)

σ: standard deviation

σ_J: standard deviation of the wave raw power (kWm^{-1})

σ_p: standard deviation of the wind raw power (kWm^{-2})

μ: average value

1. Introduction

The EU's current policy framework includes the Renewable Energy (RES) Directive (2009/29/EC), which establishes a target of 20% of renewable energy in the total energy consumption by 2020. In order to translate this general policy into concrete action, Member States are to define and publish National Renewable Energy Actions Plans indicating the mix of renewable energy technologies to be implemented. In this context, marine energy [1] has emerged as one of the most promising alternatives to fossil fuels due to the substantial resource and potential for development [2]. Among the different options, this paper is focused on offshore wind and wave energy [3] and their combination [4].

Offshore wind is admittedly more complex and costly than its onshore counterpart; however, it provides higher energy yields thanks to a combination of better resources and larger turbines, and is less contentious. The sea offers more space for deploying energy parks [5]. The installed capacity of offshore wind in the EU reached 6,562 MW at the end of 2013, producing 24 TWh in a normal wind year – enough to cover 0.7pc of the EU's electricity consumption [6]. As for wave energy, it presents extensive possibilities for the future thanks to its enormous potential for electricity production [7]. However, it is still in its infancy and the technology has a high levelised cost [8]. The inclusion of co-located Wave Energy Converters (WECs) into wind farms [9] could accelerate the development of wave energy technology, which may be expected to lead to reductions in the cost of wave energy based on the learning curve [10]. Moreover, other synergies [5] can be realised through wave and wind combined energy systems, such as cost savings by common elements [11] and coordinated strategies [12], smoothed power output [13] or a more sustainable use of the natural resources [14].

Finding suitable locations for the development of offshore parks [15] is fundamental to appeal to investors and boost the development of these novel renewables. For that purpose, not only the available resource has to be considered, the water depth or distance to land have to be assessed in a holistic way. The North Sea basin has been identified in previous studies as one of the best areas for deploying co-located farms due to the available resource and the existing shallow water [16]. Indeed, recent works such as [16] or [17] identified the Danish coast of the North Sea as a promising area for combined wind and wave energy farms. Denmark has indicated offshore wind energy targets of 1.3 GW [18] and 4.6 GW [19] by 2010 and 2025, respectively. At present, the majority of Members States have not set any targets for the development of marine energy projects in their sea basin, and therefore the elaboration of a plan for marine energy development would be a major step for progress.

The aim of this paper is to characterise the available wave and wind resource in the Danish coast to select a suitable location on the basis of the relevant factors, such as the existing wave and wind resources, water depth or distance to land. Hourly sea data from 2005 to 2015 combined with hindcasts are implemented in two numerical models: WAsP (Wind Atlas Analysis and Application Program) and SWAN (Simulating WAves Nearshore). The former is an industry-standard software for predicting the wind climate, wind resource, and power production from wind farms; and the latter is a third-generation numerical model commonly used to calculate wave generation and propagation. This paper has a second part where a co-located farm was deployed in the location identified as the optimal site in this first part with the purpose of analysing the benefits of this farm in comparison to two independent wave and wind parks.

This paper is structured in three steps. First, four case studies were defined and simulated on the basis of the available wave and wind data to determine a narrow area

suitable for co-located farms within the West Danish coast, taking into account the technical limitations of water depth and distance to coast. Second, annual series of data from February 2005 to January 2015 were run by means of numerical models to identify the best location within the previously defined area through the Co-Location Feasibility (*CLF*) index, which encompasses the available resource, power variability and correlation between waves and winds. Third, the wave and wind resources in the selected location were deeply analysed.

2. Materials and Methods

2.1. Study area

This study is focused on the West Danish coast of the North Sea (Figure 1). It is characterised by fairly long coastline and areas of shallow waters that hold great opportunities for marine energy [19]. Indeed, Denmark has the second largest amount of installed offshore wind energy capacity in Europe, behind the UK, with 1,271 MW in 2014 (19% of total European installations) [20].

Figure 1. The West Danish coast (the red framed area).

Nowadays there are technical limitations that prevent offshore installations from being installed in water depths over 50 m [21]. The vast majority of current offshore wind

farms are in water depths below 35 m – which is the limit for monopile foundations [22]. Almost the entire study area was under this limit with the exception of the NW corner (Figure 2). The distance from land is also fundamental when looking for a suitable location for it affects the capital and maintenance costs significantly. The current wind farms in the Danish coast are usually between 10-30 km away for the coastline (Figure 2).

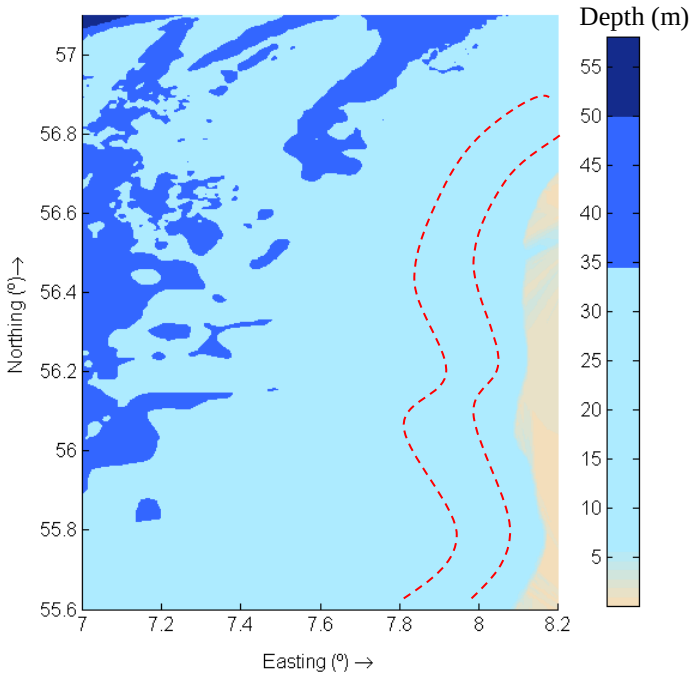

Figure 2. Bathymetry of the study area (water depth in m). The area within the red dashed lines presents distance to land between 10 and 30 km – common values in current wind farms.

2.2. Wave propagation and wind models

The wind resource assessment and wind farm calculations were carried out by means of the WAsP (Wind Atlas Analysis and Application Program) software [23], which is an implementation of the so-called wind atlas methodology [24]. The program employs a comprehensive list of models for projection of the horizontal and vertical extrapolation of wind climate statistics [25]. It is a linear numerical model based on the physical

principles of flows in the atmospheric boundary layer, and it is capable of describing wind flow over different terrains, close to sheltering obstacles and at specific points.

The available wave resource was assessed through the third-generation numerical wave model SWAN (Simulating WAves Nearshore). This model was successfully applied to examining the impact of wave farms on the wave conditions in their lee in recent studies [26]. It computes the evolution of random waves accounting for refraction, wave generation due to wind, dissipation and non-linear wave-wave interactions [27]. The model was implemented on a computational grid encompassing an area of approx. 134 km × 167 km with a resolution of 300 m × 300 m (Figure 3). Having selected the site of the co-located farm, a nested grid focused on this site was added, covering an area of 8.5 km × 8.5 km with a resolution of 17 m × 17 m. Bathymetric data from the European Marine Observation and Data Network (EMODnet) were interpolated onto this grid.

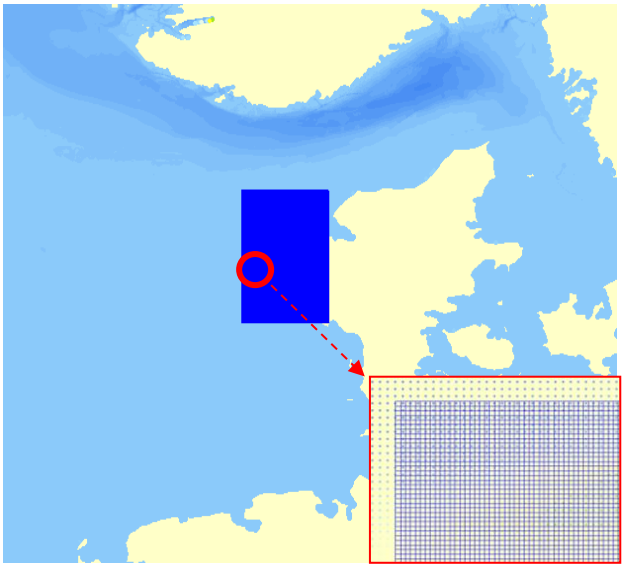

Figure 3. Computational grid (dark blue area) of the wave propagation model and a detail of its resolution.

2.3. Wave and wind data

Hindcast data from WaveWatch III, a third-generation offshore wave model, were used in conjunction with meteocean data from February 2005 to January 2015 provided by the Horns Rev wind farm in three points around the Horns Rev 3 area (Figure 4).

Figure 4. Location of the three buoys providing wave and wind data for this study.

On the basis of the annual series of data 4 case studies were defined as representative of the wind and wave climate (Table 1) for a preliminary analysis of the available resource; subsequently the complete annual series were considered.

Table 1. Definition of the four representative Case Studies (*CS*). H_{mo} = significant wave height; T_{mo1} = mean wave period; $\theta_{wave,mean}$ = mean wave direction; U_w = wind speed at 10 m above the sea level; $\theta_{wind,mean}$ = mean wind direction.

CS	H_{mo} (m)	T_{mo1} (s)	$\theta_{wave,mean}$ (°)	U_w (m/s)	$\theta_{wind,mean}$ (°)
1	1	4	330	7.5	330
2	1.5	4.5	330	9	320
3	2	5.5	320	10.5	320
4	2.5	6	330	10	330

2.4. Indicators

The available wind power (*P*) can be calculated according to the following expression [28] :

$$P = \frac{1}{2}\rho_a U_w^3 \quad (4)$$

where U_w is the wind speed, and ρ_a is the air density, assumed as equal to 1.23 kg/m^3, considering an average air temperature of 5 °C. Wind speeds are often available from meteorological observations measured at a height of 10 m. However, hub heights of offshore wind turbines are usually 40 to 80 m [29]. Eq. 5 allows the conversion of wind speed values measured at a certain height into the corresponding values at the nacelle height or any other height of interest [30]:

$$U_{w1} = U_{w2} \frac{\ln (H_1/z)}{\ln (H_2/z)} \quad (5)$$

where U_{w1} is the wind speed to be calculated at the height H_1, U_{w2} is the measured wind speed at the height H_2 and z is the roughness length.

For its part, the available wave power (J) can be determined by [31]:

$$J = \frac{\rho_w g^2}{64\pi} H_{mo}^2 T_e \quad (6)$$

where ρ_w is the sea water density (1027 kg/m^3, considering an average water salinity concentration of 33 ppm and an average water temperature of 7 °C), g is the gravity acceleration (g = 9.82 m/s^2), H_{m0} is the significant wave height, and T_e is the energy period, which is defined in terms of spectral moments as follows:

$$T_e = \frac{m_{-1}}{m_0} \quad (7)$$

where m_n represents the spectral moment of order n, which is given by:

$$m_n = \int_0^{2\pi} \int_0^{\infty} f^n E(f,\theta) df d\theta \quad (8)$$

where f is the wave frequency and $E = E(f, \theta)$ is the energy density with θ the propagation direction. The energy period can be estimated as $T_e = 1.14 T_{mo1}$ [32]

The power variability was analysed through statistical indicators such as the standard deviation (σ) or confidence intervals [33]. The variability is important for the peak-to-average ratio has been identified as a major cost driver in renewable energy systems [34]. Moreover, as considering co-located wave and wind energy farms, the analysis of the existing correlation between wave and winds is fundamental. It was determined by means of the cross-correlation factor, $c(\tau)$, (Eq. 9) [35].

$$c(\tau) = \frac{1}{N}\sum_{k=1}^{N-\tau} \frac{[x(k)-\mu_x][y(k-\tau)-\mu_y]}{\sigma_x \sigma_y} \quad (9)$$

where μ_x, μ_y and σ_x, σ_y are the mean and the standard deviation of two generic signals x and y, and τ is the time lag.

The *CLF* index (Co-location Feasibility index) (Eq. 10) was defined to balance all the above factors giving quantitative information to select the best location for a co-located farm.

$$CLF_i = \alpha_{\bar{J}} \frac{\bar{J}_i - \bar{J}_{min}}{\bar{J}_{max} - \bar{J}_{min}} + \alpha_{\bar{P}} \frac{\bar{P}_i - \bar{P}_{min}}{\bar{P}_{max} - \bar{P}_{min}} + \alpha_{c(0)} \frac{c(0)_{max} - c(0)_i}{c(0)_{max} - c(0)_{min}} + \alpha_{\sigma_{\bar{J}}} \frac{\sigma_{\bar{J},max} - \sigma_{\bar{J},i}}{\sigma_{\bar{J}max} - \sigma_{\bar{J},min}} + \alpha_{\sigma_{\bar{P}}} \frac{\sigma_{\bar{P},max} - \sigma_{P,i}}{\sigma_{\bar{P}max} - \sigma_{\bar{P},min}} \quad (10)$$

If x_i is the value of a generic parameter x at point i for the study period, x_{max} and x_{min} are the maximum and minimum values of the parameter, respectively, in the entire database. The general parameter x could correspond to the mean wave power during the study period ($\bar{J}$), the mean wind power ($\bar{P}$), the instantaneous correlation ($c(0)$) or the standard deviation of wave and wind power (σ_J and σ_P, respectively). For instance, the point with the maximum mean wave power will correspond to a value of 1 of the first term of the handside of the equation, whereas the point with the greatest power variability will

have a zero value in the last term. Different weighting factors were assigned for each parameter: $\alpha_{\bar{J}}$ and $\alpha_{\bar{P}}$ = 0.35 for the available wind and wave power − the most relevant parameters, $\alpha_{c(0)}$= 0.20 for the instantaneous correlation, and $\alpha_{\sigma_{\bar{J},\bar{P}}}$= 0.05 for the wave and wind power variability:

Having identified the best locations for a co-located wave and wind energy farm on the basis of the *CLF* index's, the assessment of the available resource was extended by analysing the wave and wind roses, the correlation between waves and winds for different time lags (τ) and the variation in the mean raw power on inter- and intra-annual time scales for the study period.

3. Results and discussion

3.1. Wind and wave model validation

The results obtained from the two models used in this study (SWAN and WAsP) were successfully validated in terms of significant wave height and wind speed, respectively, with the metocean data from February 2005 to May 2015 provided by 3 buoys around the Horns Rev 3 wind farm (Figure 4). In both cases, a good correlation was observed between the simulated and measured time series (Figure 5). This corroborated by the values of the coefficient of determination (R^2) and the Root Main Square Error (*RMSE*) (Table 2).

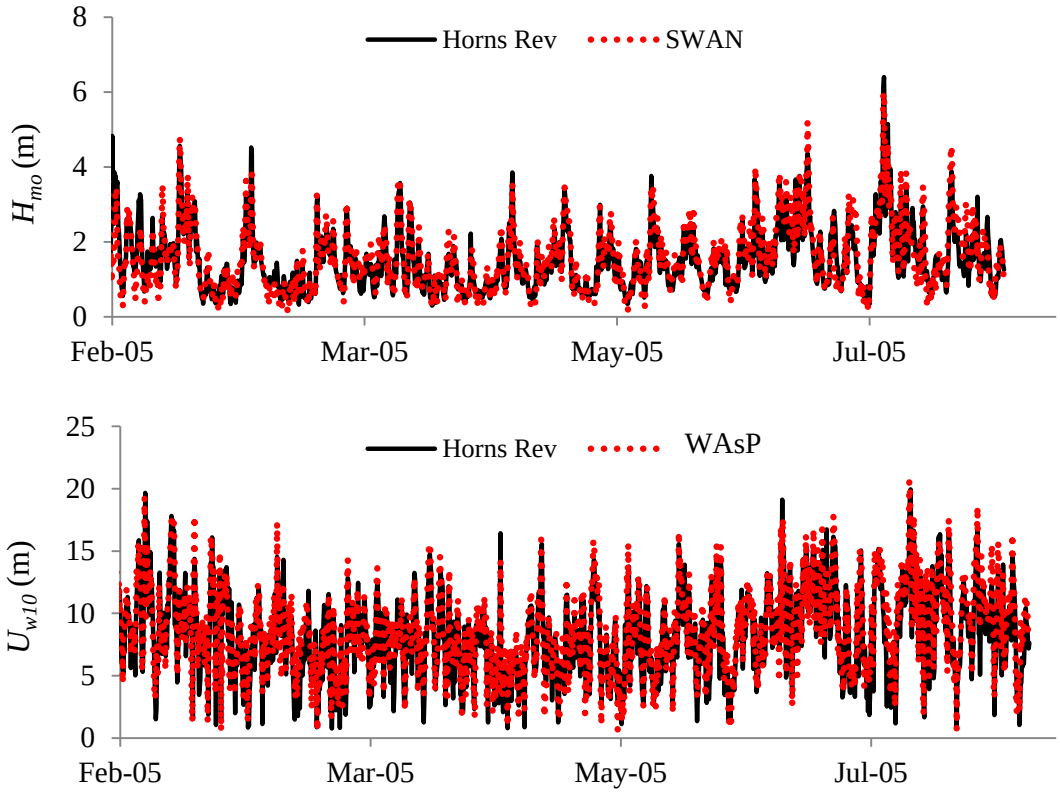

Figure 5. Correlation between hindcasts and metocean data from the buoy no.1 in the Horns Rev 3 area in terms of significant wave height (H_{mo}) and wind speed at 10 m above the sea level (U_{10m}) from February to August 2005.

Table 2. Coefficient of determination (R^2) and Root Main Square Error (*RMSE*) between hindcasts and measured significant wave height (H_{m0}) and wind speed at 10 m above the sea level (U_{10m}) from February 2005 to May 2013, for the three buoys considered.

Buoy no.	H_{m0}		U_{10m}	
	R^2	*RMSE* (m)	R^2	*RMSE* (m/s)
1	0.93	0.41	0.87	0.20
2	0.93	0.38	0.86	0.21
3	0.90	0.34	0.87	0.27

3.2. Site selection

Four representative case studies of the existing wind and wave climate (Section 2.3) were modelled to identify the best zone within the study area for deploying a co-located farm. The wind spectrum observed was quite uniform with a maximum variation by 15% from one point to another, whereas wave power presented fluctuations greater than 50% (Figure 6). It was found that in the south section of the study area it would be necessary

to move more than 30 km from shore to achieve the same wave height, and thus a similar wave power potential, as nearshore in the North section. This would obviously involve greater costs both during the farm installation and maintenance tasks. Therefore, the study of the available wave and wind resource was focused on the north section – from 56.2ºN to 56.8ºN and from 7.8ºE to 8.2ºE; 60 points where defined within this area for the analysis of the available power by means of hourly series of wave and wind data from 2005 to 2015 (Figure 7).

The 60 points analysed presented levels of wave energy above the minimum commonly suggested in the literature for offshore wave farms (4 kW/m) [36] (Table 3). The largest available wave power, $\bar{J}$, occurred at site no. 43, with a mean value over 11 kW/m. As for the wind power density, there were only small differences between the mean wind power at the 60 points analysed, with $\bar{P}$ ranging between 0.61 and 0.64 kW/m^2 (Table 3). Although the potential power production is the most important parameter when selecting the best location, there are other factors to be considered, such as the power variability. Some of the points with a large resource also had large power variability (Table 3). Nevertheless, this challenge could be overcome at some of these points thanks to the low correlation between wave and winds, which may compensate the fluctuations. If there is phase shift between them the inherent variability of the power output may be smoothed and the non-operational periods may be avoided. In terms of correlation (Table 3), site no. 30 presented the best results with an instantaneous correlation, $c\,(0)$, around 30% – a low value indeed. At the remaining points, values between 66% and 73%, were found, offering promise for co-located farms.

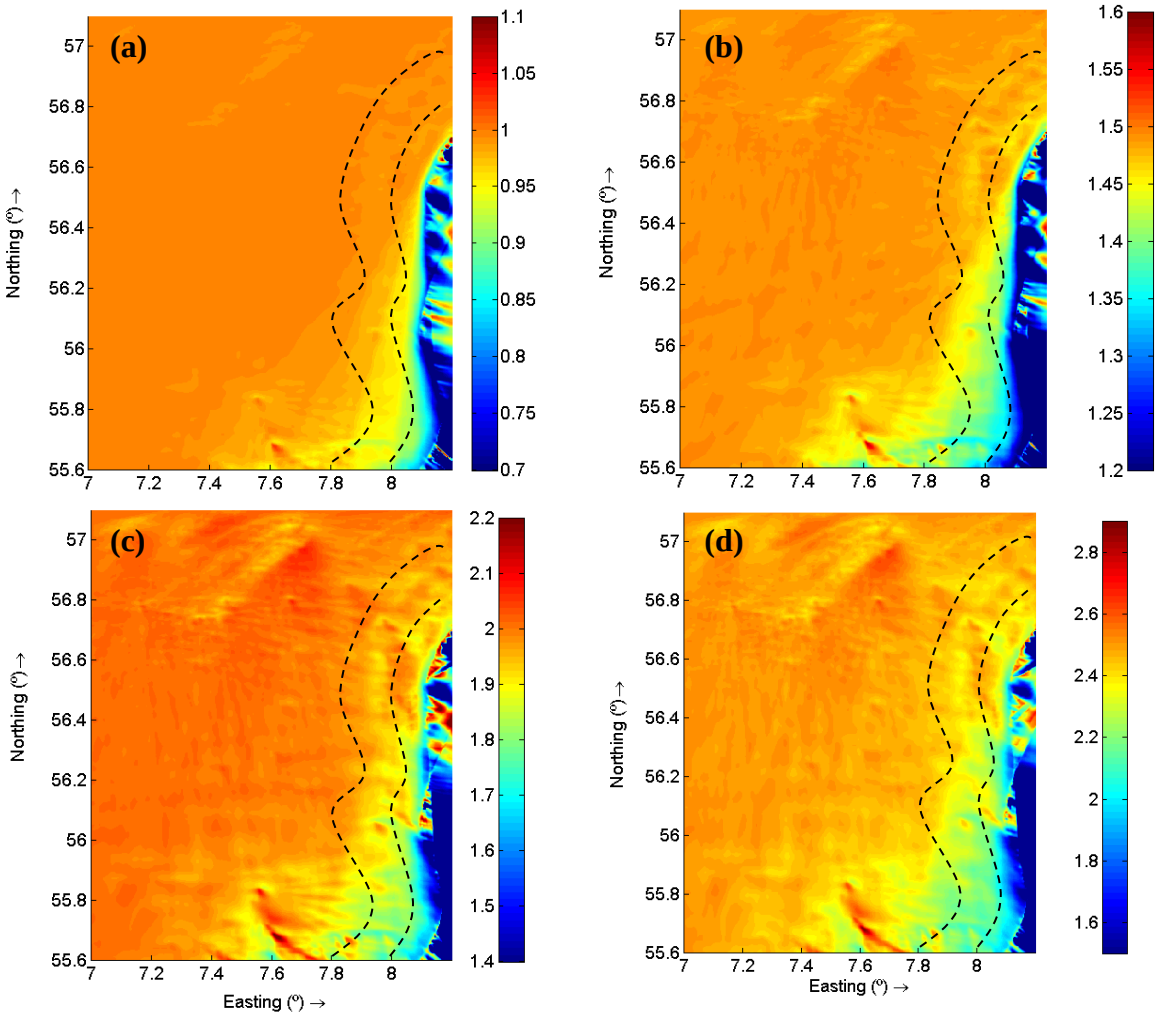

Figure 6. Significant wave height (m) within the study area for: (a) Case Study (*CS*) 1; (b) *CS* 2; (c) *CS* 3 and (d) *CS* 4. The area within the red dashed lines presents distance to land between 10 and 30 km – common values in current wind farms.

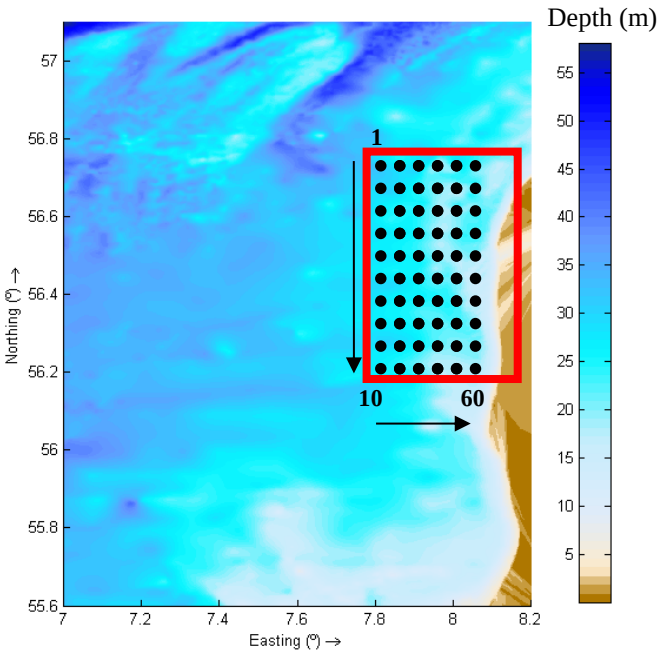

Figure 7. Bathymetry (water depth in m) of the area identified as the best location for installing a co-located farm (framed zone). The black points correspond with the 60 points were the resource was analysed – numbered from the upper right corner to the bottom left corner.

Table 3. Main statistics of wave (J) and wind (P) power: mean, median, standard deviation (σ) and 90% confidence interval (*c.i.* 90%), for 22 representative points of the total considered in this study. The instantaneous correlation c (0) between wave and wind power is also included.

Site no.	J (kW m^{-1})				P (kW m^{-2})				c (0)
	μ	Median	σ	90% c.i.	μ	Median	σ	90% c.i.	
1	11.02	4.62	17.59	0.241	0.635	0.371	0.811	0.010	0.71
4	11.35	4.63	19.14	0.262	0.626	0.372	0.814	0.012	0.72
7	11.24	4.59	18.44	0.252	0.632	0.373	0.813	0.011	0.73
10	11.31	4.61	18.78	0.257	0.631	0.372	0.812	0.011	0.73
13	10.78	4.51	17.53	0.240	0.628	0.376	0.814	0.010	0.73
16	10.95	4.42	18.43	0.252	0.631	0.374	0.816	0.009	0.72
19	10.88	4.50	18.06	0.247	0.622	0.375	0.813	0.010	0.72
20	10.94	4.47	18.34	0.251	0.631	0.373	0.811	0.012	0.73
23	10.81	4.35	18.47	0.252	0.622	0.372	0.813	0.012	0.71
26	10.42	4.25	17.51	0.239	0.623	0.373	0.814	0.010	0.72
29	10.73	4.40	18.26	0.250	0.635	0.370	0.812	0.012	0.71
30	10.78	4.33	18.49	0.253	0.627	0.372	0.809	0.011	0.33
32	10.84	4.37	18.83	0.257	0.631	0.371	0.813	0.011	0.70
35	10.70	4.25	18.71	0.256	0.625	0.372	0.812	0.011	0.71
38	10.69	4.48	17.44	0.238	0.629	0.376	0.815	0.010	0.73
41	10.51	4.30	17.21	0.235	0.628	0.374	0.811	0.012	0.70
43	11.43	4.20	21.19	0.290	0.623	0.372	0.812	0.011	0.67
46	11.28	4.13	21.42	0.293	0.618	0.373	0.813	0.011	0.66
49	10.26	4.01	17.40	0.238	0.623	0.371	0.811	0.010	0.70
52	10.17	3.95	17.75	0.243	0.621	0.370	0.814	0.012	0.71
55	10.16	3.87	18.29	0.25	0.621	0.376	0.813	0.012	0.70
58	9.52	3.68	16.98	0.232	0.631	0.375	0.812	0.011	0.69

In total, the *CLF* index value was calculated for the 60 points defined within the study area (Figure 8 and 9). The locations closer to coast present the lowest values of the *CLF* index, as well as the points located in the southern section of the study area. This is according to the distribution of the available wave and wind power analysed before. In general, the furthest locations from the coast stood up as great sites for deploying a co-located wave and wind energy farm in terms of the available resource, power variability and correlation between waves and winds. This is the general pattern; however, the location with the highest value of the *CLF* index was site no. 43 (Figures 8 and 9). This point is in the northwesterly section of the study area (Figure 8) and presents the advantage of being relatively close to land (around 8 km), which reduces installation and maintenance costs. Therefore, this site emerged as the best location for the co-located farm.

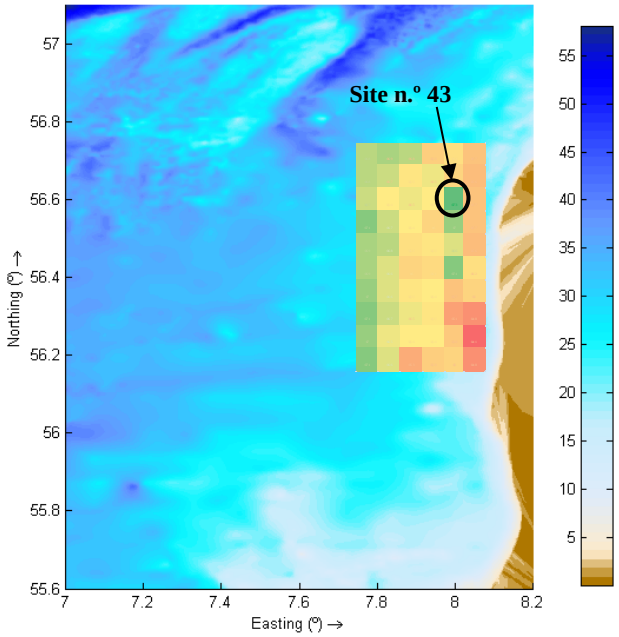

Figura 8. *CLF* index values within the study area, the green locations correspond to places with the highest values and red with the lowest ones. The colour scale corresponds to water depth in m.

Figure 9. CLF_i of the 60 sites considered in this study. The red circle indicates the site with the greatest value of the *CLF* index.

3.3. Characterisation of the selected site

The wave climate at this location was characterised by a significant wave height around 1.5 m (Table 3), and 315º as predominant wave direction (Figure 10), which also corresponded with waves with mainly contribution to the wave power (Figure 10). Waves with significant wave height over 4 m were rare, which is not a bad thing for the durability of the installation. The analysis of the wind direction (Figure 11) is also important in planning the wind farm layout. The predominant wind direction, as well as the directions with the largest contributions to the total wind resource, corresponded to westerly winds. The southeast side is sheltered by the Danish coast itself so the potential decreased clearly from this direction. The mean wind speed was around 8.7 m/s (Table 4).

Table 4. Most relevant wave and wind statistics of the site point no. 43. $\overline{H}_{mo}$: average significant wave height, $H_{m0,max}$: maximum value of the significant wave height, $\overline{T}_e$: average energy period, $T_{e,max}$: maximum energy period; $\overline{U}_{10m}$: average wind speed at 10 m above the sea level, $U_{10m,max}$: maximum wind speed at 10 m above the sea level.

Wave	$\overline{H}_{mo} \pm \sigma$ (m)	1.53 ± 1.12
	$H_{m0,max}$ (m)	9.66
	$\overline{T}_e$ (s)	5.86
	$T_{e,max}$ (s)	18.55
Wind	$\overline{U}_{10m} \pm \sigma$ (m s^{-1})	8.67 ± 3.76
	$U_{10m,max}$ (m s^{-1})	28.94

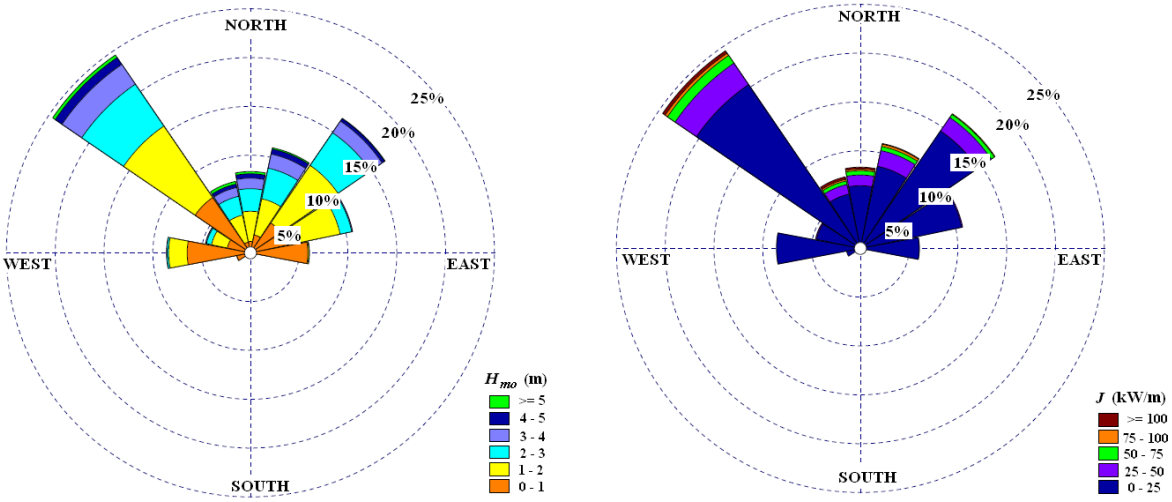

Figure 10. Wave rose (left) and wave power rose (right) for site no. 43 for the total study period (from February 2005 to January 2015).

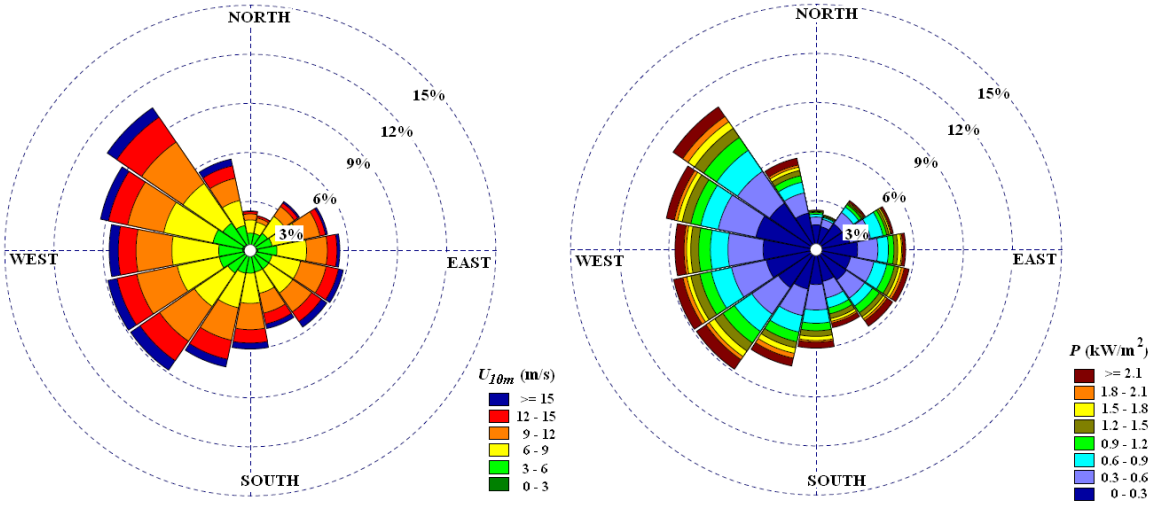

Figure 11. Wind rose (left) and wind power rose (right) for site no. 43 for the total study period (from February 2005 to January 2015).

The average wave and wind power during the study period were 11.43 kW/m and 0.64 kW/m^2, respectively. Both the inter- and intra-annual power variability are shown in Figures 12 and 13. The inter-annual variation of wave and wind power, around the mean were of 28% and 15%, respectively, was lower for both resources than the corresponding intra-annual variability, whose maximum values were 65% for wave power and 53% for wind energy. This is interesting when predicting the annual power output for the years to come. However, the intra-annual variability shows that the soft climate during spring and summer caused a clear decrease in the available power, which would translate into a low power output.

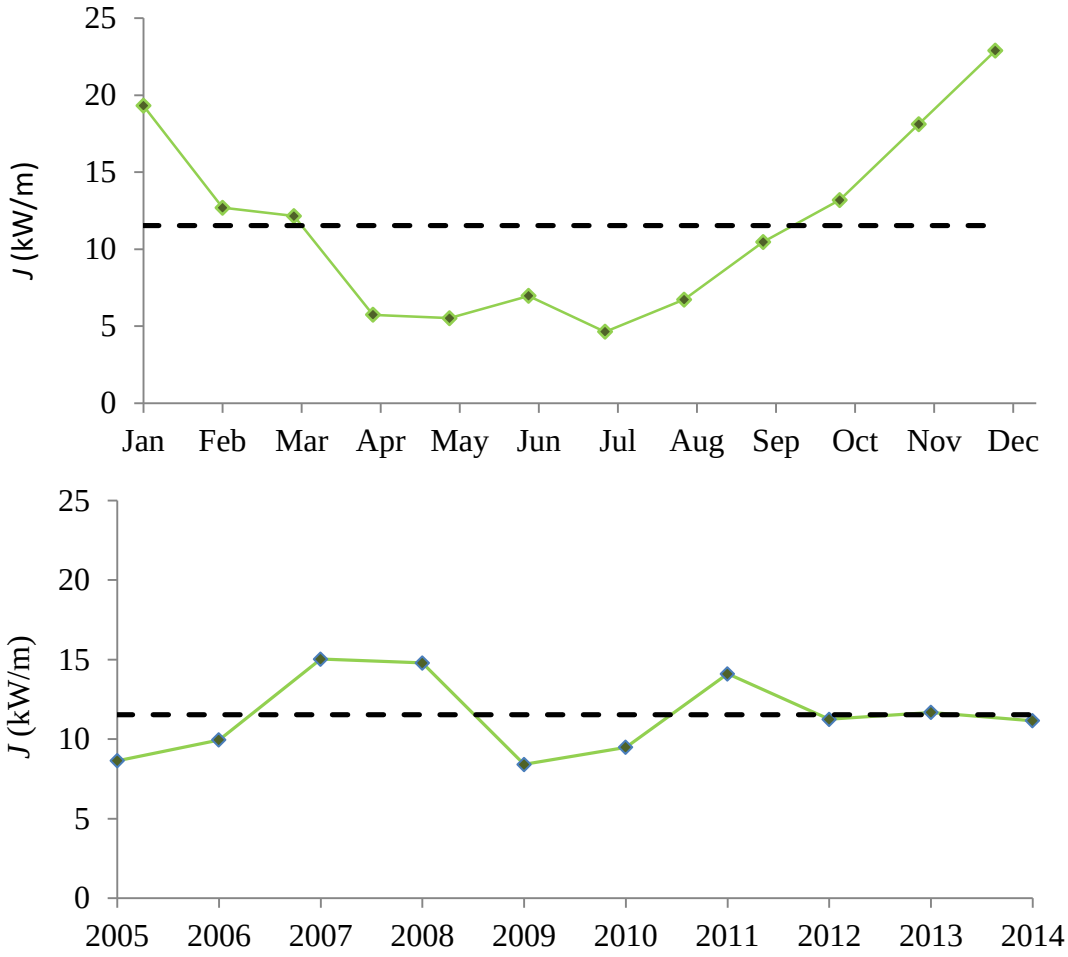

Figure 12. Variability of the mean wave power on intra- and inter-annual time scales for the study period.

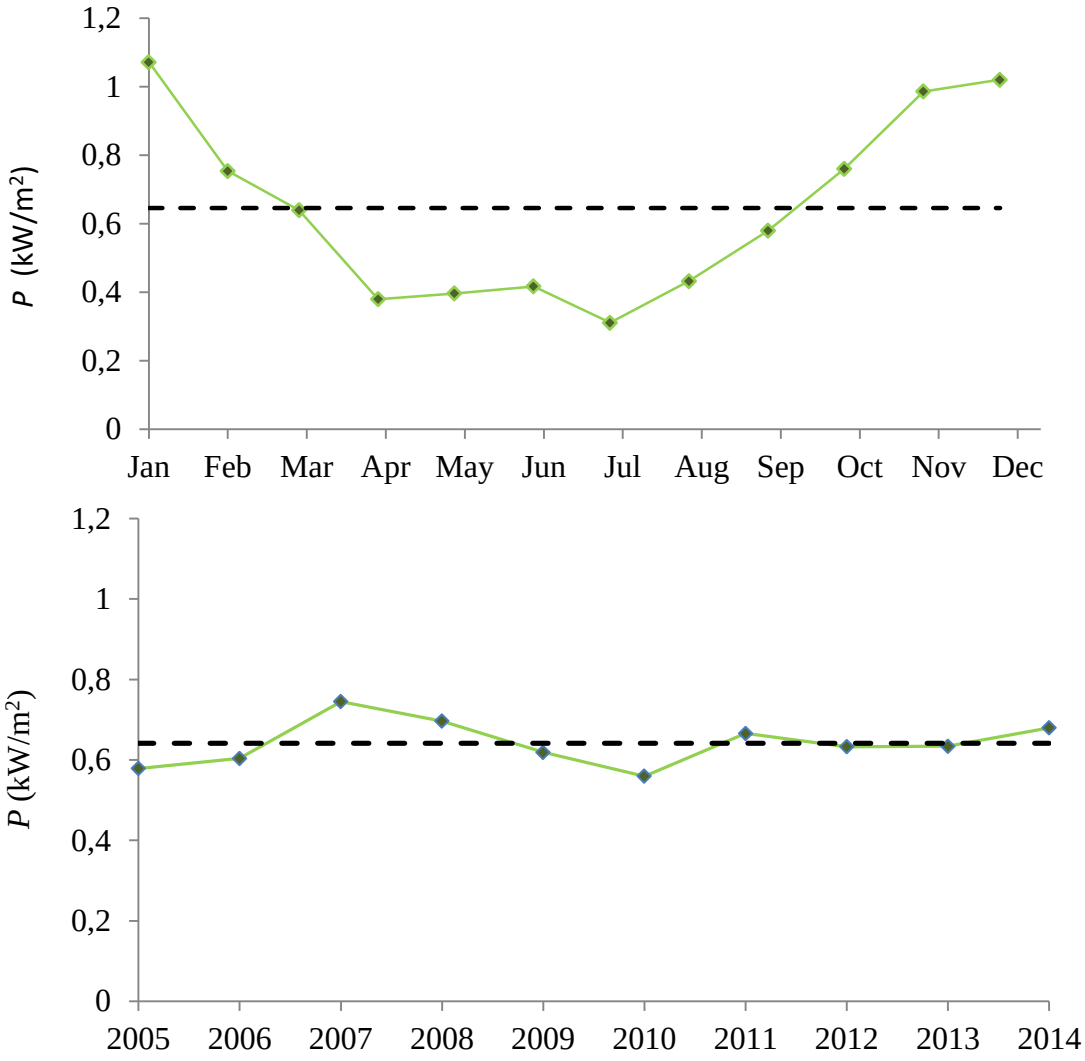

Figure 13. Variability of the mean wind power at intra- and inter-annual time scales for the study period.

For its part, the maximum value of the cross-correlation factor was obtained for a time delay of one hour (Figure 14), which demonstrated the existence of a phase shift between waves and winds that could be used to reduce the power variability and avoid non-operational periods. Moreover, the value of the instantaneous correlation, *c* (0), of 67% showed that if wind speed were out of the limits of power production, wave energy could contribute to covering the power demand during this period.

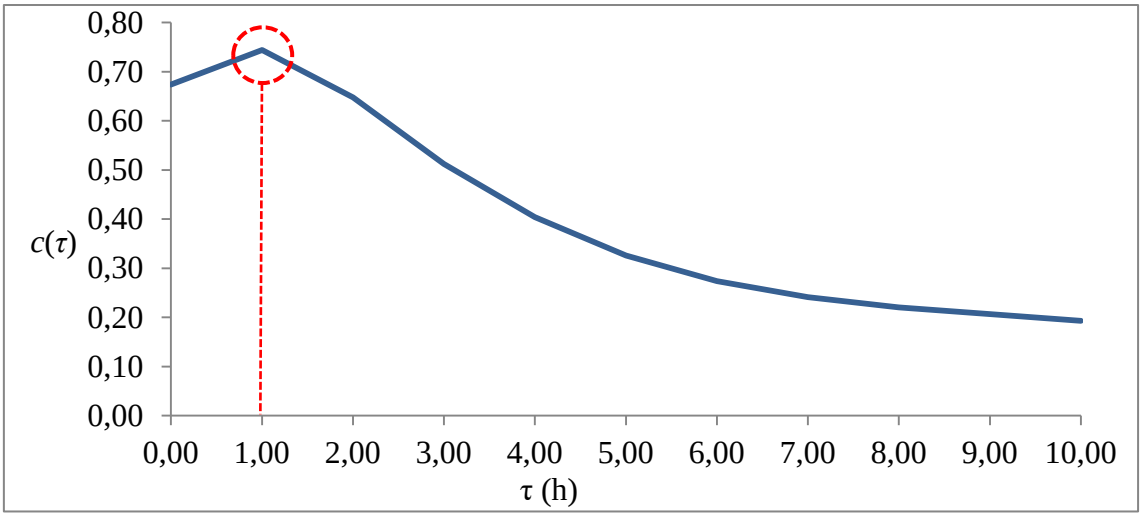

Figure 14. Correlation between wave and wind power in the site no.7 for the study period. *c(τ)* is the cross-correlation factor and *τ* the time lag.

4. Conclusions

The aim of this paper was to select the most convenient location for a co-located farm along the Danish coast, a promising area in terms of wave and wind energy. In respect of the site selection, important differences were found between the available wave resource in the north and south sections of the Danish coast. The farm would have to be located much farther offshore in the south section; therefore, the study was focused on the northern coast, where the wave and wind available resource were evaluated at 60 points. The assessment was carried out considering different factors in a holistic way byu means of the *CLF* index, which accounts for the available wave and wind power, power variability, and correlation between waves and winds; the distance from shore; and the water depth. In terms of the *CLF* index, the westerly area – the furthest from the coast – encompassed the best locations for deploying a co-located wave and wind energy farm. This is well in line with the wave and wind power distribution. However, there was a point in the northwest area, with coordinates: 56.65ºN, 8.03ºE, which presented the greatest value of the *CLF* index (0.73 over 1). Moreover, it is really near coast (8 km) and this would bring in reduced installation and maintenance costs. This

point was characterised by predominant northwesterly waves, westerly winds, and mean wave and wind power values of 11.4 kW/m and 0.64 kW/m^2, respectively. The low inter-annual variability of wave and wind power at this location would facilitate the annual power output prediction; however, the intra-annual (seasonal) variability is well marked, with weaker winds during spring and summer. The highest balancing cost due to power variability corresponds to the 15-minute variability. In this respect, the lag that was found between waves and wind. – approx. 1 hour, with a cross-correlation factor of 67% – compensated the fluctuations to some extent, effectively smoothing the power output.

In summary, it was demonstrated that the Danish coast offers favourable opportunities for co-located farms. The best site of those considered has a value of the CLF index of 0.73..

Acknowledgments

This work was carried out in the framework of the Atlantic Power Cluster project (Atlantic Area Project nr. 2011-1/151, ATLANTICPOWER), funded by the Atlantic Area Operational Transnational Programme as part of the European Regional and Development Fund (ERDF). Astariz has been supported by the FPU grant 13/ 03821 of the Spanish Ministry of Education, Culture and Sport. The authors are grateful to the Horns Rev wind farm for the resource data of the site and to the European Marine Observation and Data Network (EMODnet) for the bathymetrical data of the North Sea.

References

[1] A.S. Bahaj. 8.01 - Generating Electrical Power from Ocean Resources. in: A. Sayigh, (Ed.). Comprehensive Renewable Energy. Elsevier, Oxford, 2012. pp. 1-6.

[2] A. Vazquez, G. Iglesias. LCOE mapping: A new geospatial tool for tidal stream energy. Energy In Press. (2015).

[3] A. Al-Habaibeh, D. Su, J. McCague, A. Knight. An innovative approach for energy generation from waves. Energy Conversion and Management. 51 (2010) 1664-8.

[4] D.F. Kallesøe BS, Hansen HF and Køhler A. Prototype test and modeling of a combined wave and wind energy conversion system. Proceedings of the 8th European Wave and Tidal Energy Conference, Uppsala, Sweden, 2009.

[5] M. Veigas, G. Iglesias. Potentials of a hybrid offshore farm for the island of Fuerteventura. Energy Conversion and Management. 86 (2014) 300-8.

[6] E.T.E.W.E. Association). The European offshore wind industry -key trends and statistics 2013. Available at: http://www.ewea.org/fileadmin/files/library/publications/statistics/European_offshore_statistics_2013.pdf. (2014).

[7] P. Lenee-Bluhm, R. Paasch, H.T. Özkan-Haller. Characterizing the wave energy resource of the US Pacific Northwest. Renewable Energy. 36 (2011) 2106-19.

[8] S. Astariz, G. Iglesias. The economics of wave energy: a review. Renewable and Sustainable Energy Reviews. In Press (2015).

[9] C. Pérez-Collazo, D. Greaves, G. Iglesias. A review of combined wave and offshore wind energy. Renewable and Sustainable Energy Reviews. 42 (2015) 141-53.

[10] S. Astariz, C. Perez-Collazo, J. Abanades, G. Iglesias. Co-located wave-wind farms: Economic assessment as a function of layout. Renewable Energy. 83 (2015) 837-49.

[11] F. Caballero, E. Sauma, F. Yanine. Business optimal design of a grid-connected hybrid PV (photovoltaic)-wind energy system without energy storage for an Easter Island's block. Energy. 61 (2013) 248-61.

[12] S. Astariz, C. Perez-Collazo, J. Abanades, G. Iglesias. Co-located wind-wave farm synergies (Operation & Maintenance): A case study. Energy Conversion and Management. 91 (2015) 63-75.

[13] E.D. Stoutenburg, N. Jenkins, M.Z. Jacobson. Power output variations of co-located offshore wind turbines and wave energy converters in California. Renewable Energy. 35 (2010) 2781-91.

[14] M.M.J. Carlos. Pérez-Collazo, Hannah. Buckland , Julia. Fernández-Chozas. Synergies for a wave-wind energy concept. EWEA, Vienna, 2013.

[15] R. Carballo, G. Iglesias. A methodology to determine the power performance of wave energy converters at a particular coastal location. Energy Conversion and Management. 61 (2012) 8-18.

[16] U. Henfridsson, V. Neimane, K. Strand, R. Kapper, H. Bernhoff, O. Danielsson, et al. Wave energy potential in the Baltic Sea and the Danish part of the North Sea, with reflections on the Skagerrak. Renewable Energy. 32 (2007) 2069-84.

[17] J. Fernández-Chozas, N.E. Helstrup Jensen, H.C. Sørensen, J.P. Kofoed, A. Kabuth. Predictability of the power output of three wave energy technologies in the Danish North Sea. International Journal of Marine Energy. 1 (2013) 84-98.

[18] S. Jacques, P. Kreutzkamp, P. Joseph. Offshore Renewable Energy and Maritime Spatial Planning. Seanergy 2020 European Wind Energy Association Intelligent Energy Europe. (2011).

[19] K. Veum, L. Cameron, D.H. Hernando, M. korpås. Roadmap to the deployment of offshore wind energy in Central and Southern North Sea (2010-2030). WINDSPEED Suporting Decisions Supported by Intelligent Energy for Europe programme. (2010).

[20] http://www.4coffshore.com/windfarms/horns-rev-1-denmark-dk03.html.

[21] EWEA. Deep water. The next step for offshore wind energy. . A report by the European Wind Energy Association (EWEA) Available at: http://wwweweaorg/fileadmin/files/library/publications/reports/Deep_Waterpdf. (2013).

[22] R. Bansal, T. Bhatti, D. Kothari. On some of the design aspects of wind energy conversion systems. Energy Conversion and Management. 43 (2002) 2175-87.

[23] N. Mortensen, D. Heathfield, O. Rathmann, M. Nielsen. Wind Atlas Analysis and Application Program: WAsP 11 Help Facility. Department of Wind Energy, Technical University of Denmark, Roskilde, Denmark 366 topics. (2014).

[24] I. Troen, E. Petersen. European Wind Atlas. Risø National Laboratory, Roskilde 656 pp ISBN 87-550-1482-8. (1989).

[25] H. Frank, O. Rathmann, N. Mortensen, L. Landberg. The Numerical Wind Atlas - the KAMM/WAsP Method. Roskilde, Denmark: Riso. (2001).

[26] J. Abanades, D. Greaves, G. Iglesias. Coastal defence through wave farms. Coastal Engineering. 91 (2014) 299-307.

[27] N. Booij, Ris, R.C., Holthuijsen, L.H. A Third-Generation Wave Model for Coastal Regions 1.Model Description and Validation. J of Geophys Res. 104 (1999) 17.

[28] D.I. L. Freris. Renewable energy in power systems. John Wiley & Sons Inc (2008).

[29] D.W.I. Association. Available at: http://www.motiva.fi/myllarin_tuulivoima/windpower%20web/en/tour/wres/calculat.htm (Accessed on 20 July 2015).

[30] H.S.H.W.E. DEVELOPMENT. Environmental Impact Assessment - Noise & Vibration. Appendix 8.6 Wind Speed Calculations. Available at:

http://www.pfr.co.uk/documents/Appendix%208.6%20Wind%20Speed%20Calculations.pdf (Accessed on: 20 July 2015). (2010).

[31] D. Vicinanza, P. Contestabile, V. Ferrante. Wave energy potential in the north-west of Sardinia (Italy). Renewable Energy. 50 (2013) 506-21.

[32] Atlas of UK Marine Renewable Energy Resources. Report No. R1106. Prepared for the UK Department of Trade and Industry, ABP Marine Environmental Research Ltd. (2004).

[33] M.K. Ochi. Applied probability and stochastic processes. Wiley Inter-Science. (1990).

[34] J. Sjolte, G. Tjensvoll, M. Molinas. Power collection from wave energy farms. Applied Sciences. 3 (2013) 17.

[35] F. Fusco, G. Nolan, J.V. Ringwood. Variability reduction through optimal combination of wind/wave resources – An Irish case study. Energy. 35 (2010) 314-25.

[36] C. Brebbia, G. Benassai, G. Rodriguez. Coastal Processes. WIT Press2009.